Eur. Phys. J. B **5**, 1–5 (1998)

THE EUROPEAN PHYSICAL JOURNAL B

Shear modulus and compliance in the range of the dynamic glass transition for metallic glasses

K. Schröter[1,a], G. Wilde[2], R. Willnecker[2], M. Weiss[3], K. Samwer[3], and E. Donth[1]

[1] Fachbereich Physik, Martin-Luther-University Halle-Wittenberg, 06099 Halle (Saale), Germany
[2] Institut für Raumsimulation, DLR Köln, 51140 Köln, Germany
[3] Institut für Physik, Universität Augsburg, 86135 Augsburg, Germany

Received: 17 December 1997 / Accepted: 26 May 1998

Abstract. The dynamic shear modulus and compliance of the dynamic glass transition were investigated in two metallic glasses ($Pd_{40}Ni_{40}P_{20}$ and $Zr_{65}Al_{7.5}Cu_{17.5}Ni_{10}$). Isothermal measurements over four frequency decades enable the determination of shape parameters for the proper glass transition. The real part of the dynamic shear compliance shows a step height of approximately a factor of 2.6 for $Pd_{40}Ni_{40}P_{20}$, comparable to low molecular weight glass formers or the segmental mode as part of the glass transition in high molecular weight polymers. The frequency dependence of the imaginary part of the shear compliance at the high frequency side of the peak shows an exponent near the Andrade value of 1/3.

PACS. 64.70.Pf Glass transitions – 62.20.-x Mechanical properties of solids – 61.43.Dq Amorphous semiconductors, metals, and alloys

1 Introduction

The dynamic glass transition or α relaxation of amorphous materials appears in mechanical properties as a dramatic softening. The related temperature depends on the time scale of the experiment. For frequencies in the Hertz range and higher, the temperature range is located above the calorimetric glass transition temperature T_g in thermodynamic (metastable) equilibrium. The molecular motion responsible for the dynamic glass transition is not known and the subject of long standing controversies [1,2].

Two canonical properties of the dynamic glass transition are the non-Arrhenius temperature dependence of the related relaxation time $\tau(T)$ and the non-Debye (nonexponential) character of the relaxation curves. The former can be described by the Williams-Landel-Ferry (WLF) equation [3] or the equivalent Vogel-Fulcher-Tamman-Hesse (VFTH) equation [4]

$$\log \tau = \log \tau_0 + \frac{B}{T - T_\infty} \tag{1}$$

where τ_0 is a microscopic relaxation time (the high-temperature asymptote) and T_∞ the Vogel temperature. A measure of this non-Arrhenius character is the fragility parameter [5,6]

$$m = \frac{d \log \tau}{d(\frac{T_g}{T})} \mid_{T=T_g} . \tag{2}$$

For small temperature differences equation (1) can be approximated by the Arrhenius equation

$$\log \tau = \log \tau_0 + \frac{E_A}{\ln 10 \cdot R \cdot T} \tag{3}$$

with R the universal gas constant and E_A an apparent activation energy. With equation (3) one gets from equation (2) [6]

$$m = \frac{E_A(T_g)}{\ln 10 \cdot R \cdot T_g} . \tag{4}$$

The nonexponentiality is often described by the Kohlrausch-Williams-Watts (KWW) function (stretched exponential) [7,8]

$$x(t) = x(0) \exp \left[- \left(\frac{t}{\tau} \right)^\beta \right] . \tag{5}$$

$x(t)$ means here a relaxation property like the shear relaxation modulus $G(t)$ and β is the KWW-exponent. For measurements in the frequency domain often the Havriliak-Negami function [9] is used. In contrast to the KWW function it contains two shape parameters b and g.

In low molecular weight glass formers the dynamic glass transition is intimately connected to the onset of flow. The temperature dependence of the shear viscosity η parallels that of the α relaxation time τ. For times $t > \tau$ the shear modulus is dominated by the Newtonian flow. The complex shear compliance $J^* = J' - i \cdot J''$

$$J'(\omega) - i \cdot J''(\omega) = \frac{1}{G'(\omega) + i \cdot G''(\omega)} \tag{6}$$

[a] e-mail: k.schroeter@physik.uni-halle.de

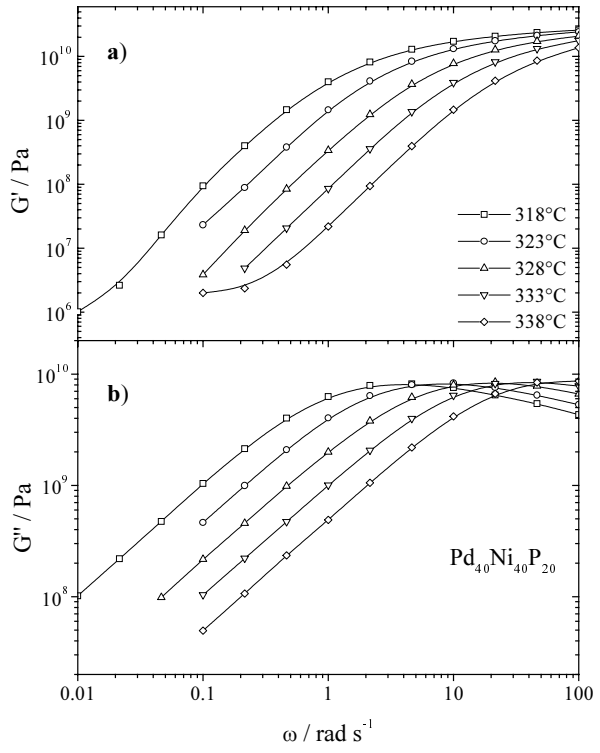

Fig. 1. Frequency dependence of (a) the real part and (b) the imaginary part of the shear modulus of $Pd_{40}Ni_{40}P_{20}$ for different temperatures.

is better suited to describe the flow characteristics than the shear modulus $G^* = G' + i \cdot G''$ because the imaginary part J'' includes the flow explicitly as an additive term and the real part J' not at all [10,11].

$$J'(\omega) = J_g + \int_{-\infty}^{\infty} L(\ln\tau)\frac{1}{1+(\omega\tau)^2} d\ln\tau \qquad (7)$$

$$J''(\omega) = \frac{1}{\omega\eta} + \int_{-\infty}^{\infty} L(\ln\tau)\frac{\omega\tau}{1+(\omega\tau)^2} d\ln\tau. \qquad (8)$$

The function $L(\ln\tau)$ contains the information on the shape and strength of the relaxation part (anelastic part) and is called retardation spectrum.

Plazek showed for different organic low molecular weight glass formers that the step in J' between the short time value on the glass side J_g and the long time value J_e^0 on the liquid side corresponds to a factor of 2.4-3.4 [12]. This (and not the dramatic decrease of the modulus by three or more orders of magnitude, see Fig. 1) corresponds to the relaxation part of the dynamic glass transition. Duffrene *et al.* [13] called this factor a viscoelastic constant $\langle\tau_1^2\rangle / \langle\tau_1\rangle^2$ and found a value of 2.62 for a soda-lime-silica glass in shear. For low molecular weight polystyrene Plazek found a factor of four [14,15] and for poly(methylphenylsiloxane) [16] a factor of five.

In high molecular weight polymers the flow motion of the long chains is hindered because they cannot cross each other. This so-called entanglement effect causes a plateau in the real part of shear modulus or compliance on longer time scales than the dynamic glass transition. The step in shear compliance between the glass value and this plateau typically amounts to two to three orders of magnitude. This whole dispersion zone was traditionally ascribed to the dynamic glass transition or main transition in polymers [17].

Detailed measurements on high molecular weight polymers identified a small contribution in J or the spectrum L on the high frequency side of the main transition (the region of the G'' peak) [18–20]. The main transition is envisaged as composed of different contributions with even different temperature dependencies [14,21,22]. The small contribution was interpreted as the proper glass transition [22] analogously to the small step in low molecular weight glass formers. Based on this experiments, the step height in J' for the proper glass transition in high molecular weight polystyrene was estimated [23] and also a factor of four was found. Apparently, structurally very different glass formers show similar values for the strength ΔJ of the proper glass transition.

With the appearance of metallic glasses with a wide supercooled liquid region [24–26] detailed mechanical measurements in the main transition region became possible [27]. Creep measurements showed KWW-exponents very similar to other strong glass formers [28,29]. The temperature dependence of viscosity could be determined [30] but the anelastic contribution to the whole relaxation could only qualitatively estimated [31]. Dynamic measurements showed the dependence of the modulus from temperature in the glass transition zone [32,33]. But no isothermal measurements over a broad frequency range were done. Crystallization intervened before flow was reached. Shear compliances were not estimated.

The purpose of this work is to determine, for the first time, the isothermal shear modulus and shear compliance in a broad frequency interval in the glass transition region for bulk metallic glasses. The step height of the shear compliance is estimated and compared to other classes of glass formers. This should contribute to a better understanding of the basic properties of the glass transition in different molecular systems.

2 Experimental

$Pd_{40}Ni_{40}P_{20}$ samples were prepared by alloying premelted Ni_2P samples (99.5% pure) with a Pd ingot (99.95% pure) in a resistance furnace under argon atmosphere. Following this prealloying treatment, the resulting ingots were cleaned in a B_2O_3 flux. After carefully removing the flux, the fully amorphous samples were produced by die casting into a cooled copper mold under argon atmosphere. The given compositions are atomic per cents.

Analogously, the $Zr_{65}Al_{7.5}Cu_{17.5}Ni_{10}$ samples were prepared using the appropriate amount of pure elements (Zr 99.935%, Al, Cu 99.999% (5N), Ni 99.99% (4N+), $O_2 < 60$ ppm). For details see [27]. They melt was cast

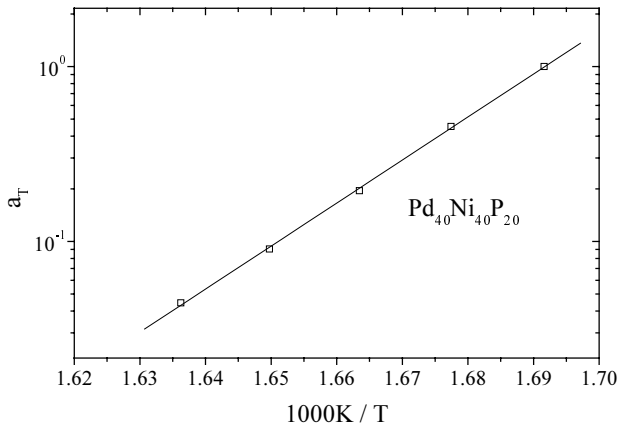

Fig. 2. Horizontal shift factors for $Pd_{40}Ni_{40}P_{20}$ estimated from the modulus curves in Figure 1. The reference temperature was 318 °C.

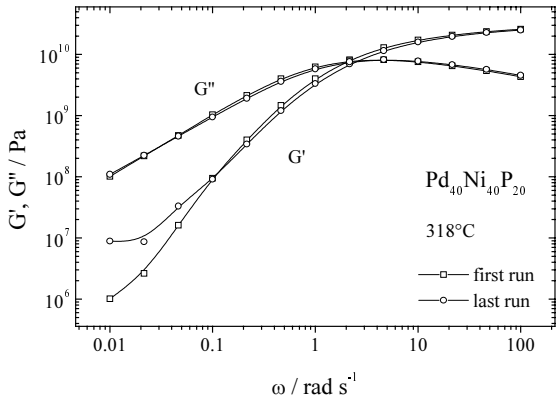

Fig. 3. Comparison of the first (□) and last (○) measurement run at 318 °C.

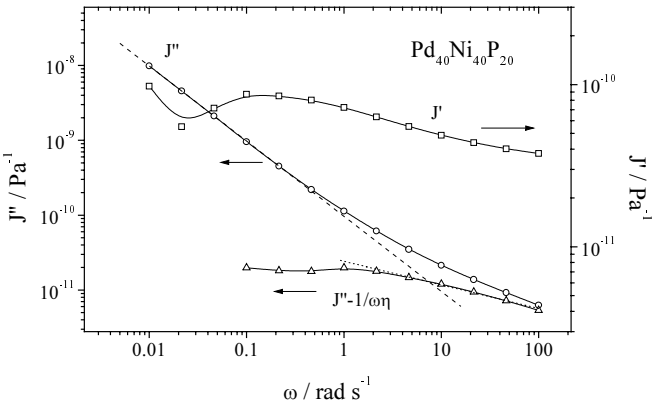

Fig. 4. Real (□) and imaginary (○) part of the complex shear compliance of $Pd_{40}Ni_{40}P_{20}$ for a temperature of 318 °C. The dashed line is a linear fit based on the imaginary part J'' at the lowest frequencies. The imaginary part corrected for the flow contribution is also shown (△). The dotted line is a linear fit on the high frequency side of this anelastic contribution.

into a cooled copper mould. The amorphous structure of the samples was confirmed by wide angle X-ray scattering.

Two stripes were cut from each sample for the mechanical measurements with the help of a diamond wire saw. The final samples had dimensions of approximately 1.5–2 mm thickness, 5.5 mm width and 20 mm length.

Shear modulus was investigated with a mechanical spectrometer RDA II from Rheometrics Scientific in a frequency range from 0.01 to 100 rad/s. Only three frequency points per decade were taken to shorten the measurement time and minimize time for interfering crystallization. The strain in the sample was 0.01% well within the linear deformation range. The shear compliance was calculated from the modulus by $G^* \cdot J^* = 1$.

The measurements started with the lowest temperature and highest frequency. After accomplishment of all isothermal measurements the run with the first temperature was repeated to check for crystallization effects. All measurements were done under a nitrogen gas stream.

3 Results and discussion

Figure 1 shows the frequency dependence of the shear modulus of $Pd_{40}Ni_{40}P_{20}$ for different temperatures. The broad maximum in G'' corresponds to the dynamic glass transition. At low frequencies the curves approach the slope one for G'' and two for G'. Both correspond to Newtonian flow. One should recognize the strong variation of the modulus values over four orders of magnitude. The upturn of G' at the highest temperature and lowest frequencies is a hint at the beginning of structural ordering which hinders the flow motion. The dispersion curves resemble those of anorganic glasses [34,35].

All curves can be superimposed by a horizontal shift to form a mastercurve (not shown). This means that the time-temperature superposition principle is valid. The corresponding shift factors are depicted in Figure 2. An apparent Arrhenius behavior is found over a small temperature range. In the temperature window of the experiments the curvature of the VFTH curve is not detectable. Due to the unphysically low value of $\tau_0 = 10^{-42}$ s for the extrapolated high temperature relaxation time (attempt frequency) and the high value of $E_A = 471$ kJ/mol for the apparent activation energy a pronounced curvature over greater temperature ranges is expected. This is typical of cooperative relaxation processes.

Usually T_g is defined from calorimetric experiments with typical frequencies of about 1 mHz. To avoid extrapolation we use the temperature where the maximum in G'' is at 1 Hz. Equation (4) then gives a fragility parameter $m(1\text{ Hz}) = 41.5$. This value is comparable with fragility parameters from literature [27,36] concerning the fact that T_g is frequency dependent.

Figure 3 compares the first run at 318 °C with the last run taken after accomplishment of all isothermal measurements at higher temperatures. The curves compare very well except at the lowest frequencies in the flow region where first crystallization effects become visible.

Figure 4 shows the frequency dependence of the dynamic shear compliance of $Pd_{40}Ni_{40}P_{20}$ at a temperature of 318 °C. The imaginary part at low frequencies is

Table 1. Apparent activation energy E_A, Newtonian viscosity η, values of shear compliance J_g on the glass side and J_e^0 on the liquid side of the glass transition, frequency location of the maxima of G'' and $J'' - 1/\omega\eta$, full frequency width at half maximum of the G" peak, Andrade exponent from $J'' - 1/\omega\eta$, fragility m.

metallic glass	$Pd_{40}Ni_{40}P_{20}$ (318 °C)	$Zr_{65}Al_{7.5}Cu_{17.5}Ni_{10}$ (371 °C)
apparent E_A in kJ/mol	471 ± 6	555
η in GPa s	10 ± 2	210
$J_g = 1/G_g$ in GPa^{-1}	$(3.5 \pm 0.2) \times 10^{-2}$	$(3.85s \pm 0.2) \times 10^{-2}$
J_e^0 in GPa^{-1}	$(9 \pm 2) \times 10^{-2}$	-
$\omega_{\max,G''}$ in rad/s	$\sim$4	$\sim$0.1
$\omega_{\max,J_r''}$ in rad/s	$\sim$1	$\sim$0.2
$FWHM$ of G'' in decades	2.4	2.2
$d \log J_r''/d \log \omega$	-0.33 ± 0.015	-0.378 ± 0.004
m at 1 Hz	41.5 ± 1	43 ± 1

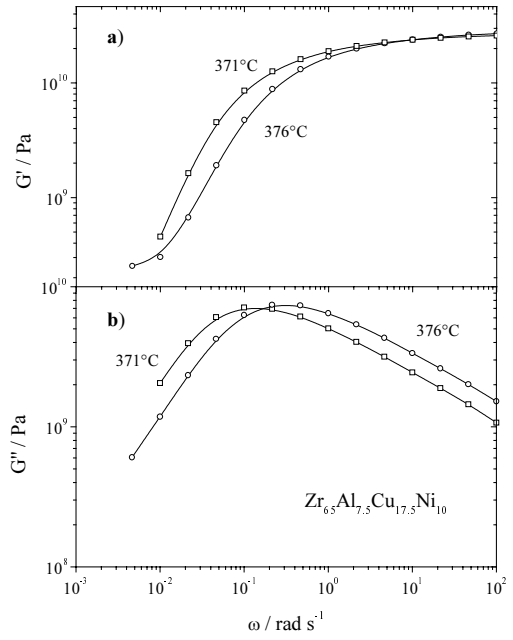

Fig. 5. Frequency dependence of (a) the real part and (b) the imaginary part of the shear modulus of $Zr_{65}Al_{7.5}Cu_{17.5}Ni_{10}$ for temperatures of 371 and 376 °C.

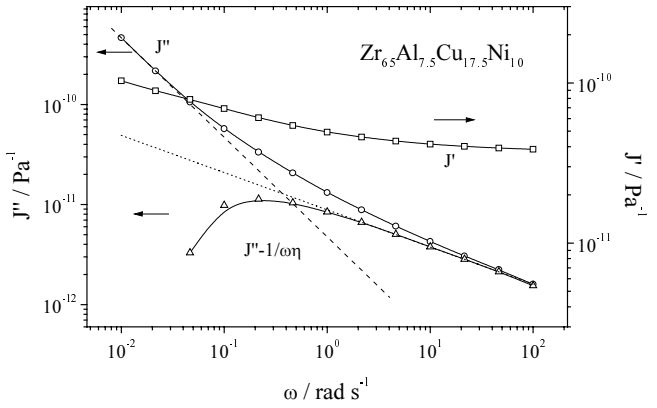

Fig. 6. Real (□) and imaginary (○) part of the complex shear compliance of $Zr_{65}Al_{7.5}Cu_{17.5}Ni_{10}$ for a temperature of 371 °C. The dashed line is a linear fit on the imaginary part J'' at the lowest frequencies. The imaginary part corrected for the flow contribution is also shown (△). The dotted line is a linear fit on the high frequency side of this anelastic contribution.

dominated by the flow term in equation (8). From the slope of this line a viscosity of 1.07×10^{10} Pa s was determined. From measurements of the equilibrium viscosity of the deeply undercooled melt of this alloy, covering almost nine decades between 10^5 Pa s and 10^{14} Pa s [37,38], a value of 4×10^9 Pa s at 318 °C was obtained.

After subtraction of the flow term from J'' the remaining relaxation part $J_r'' = J'' - 1/\omega\eta$ shows the expected shallow maximum. The corresponding increase can be found in the real part J'. The upturn in J_r'' at low frequencies and the corresponding scatter in J' are caused by uncertainties in the measurement values and beginning short range ordering [39]. Nevertheless an increase in J' between a glass value J_g of approximately 3.5×10^{-11} Pa^{-1} and a value J_e^0 on the liquid side around 9×10^{-11} Pa^{-1} can be found. This corresponds to a factor of 2.6, in agreement to the values for the glass forming organic liquids and anorganic glasses. All estimated values are collected in Table 1.

A fit of the high frequency side of the J_r'' peak to a linear function gives a slope of approximately 0.33. This corresponds to an exponent 1/3 called Andrade creep [40] commonly found on the short time side of the dynamic glass transition in high molecular weight polymers [41] or low molecular weight organic liquids [12]. On the low frequency side of the peak the uncertainty is to great to draw any conclusions about characteristic exponents.

Figure 5 shows the dynamic moduli in the main transition range for the other metallic glass $Zr_{65}Al_{7.5}Cu_{17.5}Ni_{10}$, analogously to Figure 1. Only measurements at two temperatures could be taken because crystallization interfered sooner. One should recognize the more expanded scale for the moduli compared to Figure 1. Nevertheless, also in this case the dynamic glass transition and subsequently Newtonian flow can be found.

From the temperature shift factor an activation energy of 555 kJ/mol was estimated. This is slightly higher than values from calorimetry (415-535 kJ/mol) [30]. Analogously to the other metallic glass here a fragility of $m(1\,\mathrm{Hz}) = 43$ was estimated. Both substances show only a minor difference in this value and so no conclusions about correlations of physical parameters and fragility can be drawn within experimental accuracy.

Figure 6 shows the corresponding curves for the dynamic compliance J^* at a temperature of 371 °C. The real part J' at low frequencies seems to increase above 10^{-10} Pa s. An unambiguous determination of the step height in J' was not possible.

A linear fit to the $\log J''(\log \omega)$ curve at low frequencies yielded a viscosity of 2.1×10^{11} Pa s. This is comparable to a value of $\sim 7 \times 10^{10}$ Pa s read from Figure 3 in reference [30]. With the viscosity the anelastic contribution $J''_r = J'' - 1/\omega\eta$ was separated. Again a broad peak with a slope of 0.38 on the high frequency side similar to Andrade creep was found.

4 Conclusions

Measurements of the dynamic (complex) shear modulus and shear compliance in a broad frequency interval in the glass transition region for bulk metallic glasses are presented for the first time. In the shear compliance, the flow contribution could be subtracted and the relaxation contribution of the proper glass transition is determined. It corresponds to a step ratio J_e^0/J_g in the real part of the shear compliance of about 2.6 for $Pd_{40}Ni_{40}P_{20}$. This is a value similar to low molecular weight organic liquids or high molecular weight polymers. Apparently, structurally very different glass formers show similar values for the strength of the proper glass transition.

The frequency dependence of shear compliance shows an Andrade exponent 1/3. Obviously, the shear retardation spectrum of metallic glasses, analogously to low molecular weight glass formers, consists of only one long Andrade flank without any pronounced peak opposite to the case of polymers.

Financial support by the Deutsche Forschungsgemeinschaft (DFG) and the Fonds der Chemischen Industrie (FCI) is gratefully acknowledged.

References

1. See *e.g. Alicante Conference on Relaxations in Complex Systems*, edited by K.L. Ngai, G.B. Wright, 1993 [J. Non-cryst. Solids **172-174** (1994)].
2. E. Donth, *Relaxation and Thermodynamics in Polymers. Glass Transition* (Berlin, Akademie 1992).
3. M.L. Williams, R.F. Landel, J.D. Ferry, J. Amer. Chem. Soc. **77**, 3701 (1955).
4. H. Vogel, Phys. Z. **22**, 645 (1921); G.S. Fulcher, J. Ceram. Soc. **8**, 339 (1925); G. Tammann, W. Hesse, Z. Anorg. Allg. Chem. **156**, 245 (1926).
5. C.A. Angell, in *Relaxations in Complex Systems*, edited by K.L. Ngai, G.B. Wright (Springfield, VA: National Technical Information Service, US Department of Commerce, 1985), p. 3.
6. I.M. Hodge, J. Non-cryst. Solids **202**, 164 (1996).
7. R. Kohlrausch, Ann. Phys. (Leipzig) **12**, 393 (1847).
8. G. Williams, D.C. Watts, Trans. Faraday Soc. **66**, 80 (1970).
9. S. Havriliak, S. Negami, Polymer **8**, 161 (1967).
10. F.R. Schwarzl, L.C.E. Struik, Adv. Mol. Relax. Proc. **1**, 201 (1967).
11. D.J. Plazek, J. Rheol. **36**, 1671 (1992).
12. D.J. Plazek, C.A. Bero, I.-C. Chay, J. Non-Cryst. Solids **172**, 181 (1994).
13. L. Duffrene, R. Gy, J. Non-Cryst. Solids **211**, 30 (1997).
14. K.L. Ngai, D.J. Plazek, J. Rubber Chem. Technol. **68**, 376 (1995)
15. D.J. Plazek, V.M. O'Rourke, J. Polym. Sci., Part A-2 **9**, 209 (1971).
16. D.J. Plazek, C. Bero, S. Neumeister, G. Floudas, G. Fytas, Colloid Polym. Sci. **272**, 1430 (1994).
17. J.D. Ferry, *Viscoelastic Properties of Polymers* (New York, Wiley 1980)
18. D.J. Plazek, Polym. J. **12**, 43 (1980).
19. D.L. Plazek, D.J. Plazek, Macromol. **16**, 1469 (1983).
20. S. Reissig, M. Beiner, J. Korus, K. Schröter, E. Donth, Macromol. **28**, 5394 (1995).
21. E. Donth, K. Schneider, Acta Polym. **36**, 273, 213 (1985).
22. E. Donth, M. Beiner, S. Reissig, J. Korus, F. Garwe, S. Vieweg, S. Kahle, E. Hempel, K. Schröter, Macromol. **29**, 6589 (1996).
23. K.L. Ngai, D.J. Plazek, I. Echeverrier, Macromol. **29**, 7937 (1996).
24. A. Inoue, T. Zhang, T. Masumoto, J. Non-Cryst. Solids **150**, 396 (1992).
25. A. Peker, W.L. Johnson, Appl. Phys. Lett. **63**, 2342 (1993).
26. K.C. Chow, S. Wang, H.W. Kui, J. Appl. Phys. **74**, 5410 (1993).
27. R. Rambousky, M. Moske, K. Samwer, Z. Phys. B **99**, 387 (1996).
28. M. Weiss, M. Moske, K. Samwer, Appl. Phys. Lett. **69**, 3200 (1996).
29. W. Ulfert, H. Kronmüller, J. Phys. IV France **6**, 617 (1996).
30. J. Zappel, F. Sommer, J. Non-Cryst. Solids **207**, 494 (1996).
31. K. Russew, P. de Hey, J. Sietsma, A. van den Beukel, Acta Mater. **45**, 2129 (1997).
32. R. Rambousky, M. Moske, K. Samwer, Mater. Sci. Forum **179-181**, 761 (1995).
33. H. Kimura, A. Inoue, N. Nishiyama, K. Sasamori, O. Haruyama, T. Masumoto, Sci. Rep. RITU A **43**, 101 (1997).
34. L. Donzel, R. Schaller, J. Phys. IV France **6**, 663 (1996).
35. L. Duffrene, R. Gy, H. Burlet, R. Piques, A. Faivre, A. Sekkat, J. Perez, Rheol. Acta **36**, 173 (1997).
36. R. Böhmer, K.L. Ngai, C.A. Angell, D.J. Plazek, J. Chem. Phys. **99**, 4201 (1993).
37. G. Wilde, G.P. Görler, R. Willnecker, S. Klose, H.J. Fecht, Mater. Sci. Forum **225-227**, 101 (1996).
38. G. Wilde, Ph.D Thesis, University of Berlin, 1997.
39. H. Schumacher, U. Herr, D. Oelgeschlaeger, A. Traverse, K. Samwer, J. Appl. Phys. **82**, 155 (1997).
40. E.N. da C. Andrade, Philos. Mag. **7**, 2003 (1962).
41. D.J. Plazek, E. Riande, H. Markovitz, N. Raghupathi, J. Polym. Sci., Polym. Phys. Ed. **17**, 2189 (1979).